



Numerical Heat Transfer, Part A: Applications

An International Journal of Computation and Methodology

ISSN: 1040-7782 (Print) 1521-0634 (Online) Journal homepage: <https://www.tandfonline.com/loi/unht20>

A numerical investigation on dynamics of ferrofluid droplet in nonuniform magnetic field

Kong Ling, Kai-Kai Guo, Shuai Zhang & Wen-Quan Tao

To cite this article: Kong Ling, Kai-Kai Guo, Shuai Zhang & Wen-Quan Tao (2019) A numerical investigation on dynamics of ferrofluid droplet in nonuniform magnetic field, Numerical Heat Transfer, Part A: Applications, 75:10, 690-707, DOI: [10.1080/10407782.2019.1609277](https://doi.org/10.1080/10407782.2019.1609277)

To link to this article: <https://doi.org/10.1080/10407782.2019.1609277>



Published online: 06 Jun 2019.



Submit your article to this journal [↗](#)



Article views: 14



View Crossmark data [↗](#)



A numerical investigation on dynamics of ferrofluid droplet in nonuniform magnetic field

Kong Ling^{a,b}, Kai-Kai Guo^c, Shuai Zhang^{a,b}, and Wen-Quan Tao^a

^aKey Laboratory of Thermo-Fluid Science & Engineering of MOE, Xi'an Jiaotong University, Xi'an, China; ^bXi'an ShuFeng Technological Information, Ltd, Xi'an, China; ^cState Key Laboratory of Multiphase Flow in Power Engineering, Xian Jiaotong University, Xian, China

ABSTRACT

This article presents a 3D numerical investigation on ferrofluid droplet motion in magnetic field using VOSET. A nonuniform magnetic field mimicking the one produced by an electric wire loop was generated in a finite computational domain. A validation problem on droplet deformation in uniform magnetic field was first studied, and it gives consistent aspect ratios with reported experiments. The simulation revealed an entire process of the ferrofluid droplet movement, and the influences by the intensity of the magnetic field was investigated and analyzed. Finally, a set of simulations were conducted for net magnetic force on spherical droplet, and the achieved data led to a correlation, which gives accurate prediction in the magnitude of the magnetic force and can be applied to droplet with a certain degree of deformation.

ARTICLE HISTORY

Received 19 February 2019
Accepted 15 April 2019

1. Introduction

Ferrofluid is an artificial synthesized colloidal suspension of magnetic nanoparticles coated with a surfactant dispersed in a carrier fluid [1]. The magnetic particles are small enough in scale (3–15 nm) such that Brownian motions can prevent them from settling. The composition of ferrofluid makes it a magnetic medium with fluidity.

When exposed to external magnetic field, ferrofluid takes on many interfacial phenomenon due to the effect of Maxwell stress. The most famous ones among them are Rosensweig instability [2] where the interface deforms into convexes and concaves arranged in a regular manner, and labyrinthine instability [3] where the ferrofluid deforms into highly branched structures. The unique properties of ferrofluid lead to a wide range of applications, such as micro pump [4–6], fluid seal [7, 8], energy harvester [9], drug delivery [10], and eye surgery [11]. Most of the applications of ferrofluid are achieved by non-contact control of droplet through variations of external magnetic field. However, the flow behavior and mechanism of ferrofluid droplets have not been fully understood.

With the development of numerical methods and the improvement of computer performance, numerical simulation is becoming an increasingly important tool to study the behavior of ferrofluid droplet under magnetic fields and to further reveal the coupling mechanism of magnetic field and flow field. Due to the complexity of the issues of two-phase flow under magnetic field,

the corresponding numerical methods are still in development. A brief review in this regard is presented below.

A VOF type code was developed and tested by Korlie et al. [12] to study the dynamics of ferrofluid droplets in the presence of uniformly imposed magnetic fields.

Ki [13] proposed a computational approach for simulating ferrofluid free surface flows based on Level-set method. The numerical methods were tested by two-dimension calculations on droplet falling and bubble rising for the validity and effectiveness. Although the medium studied is liquid metal rather than ferrofluid, the mechanism of coupling magnetic field and flow field is the same.

Habera and Hron [14] proposed a numerical approach based on finite element method to solve the Maxwell's equations for ferrofluid free surface flows. Equilibrium droplet shapes were numerically studied as the test and the results were compared with experiments.

Afkhami et al. [15] simulated the motion and deformation of ferrofluid droplet placed in the nonmagnetic fluid in presence of nonuniform magnetic field. The numerical simulation used a volume-of-fluid algorithm with a continuum-surface-force formulation for an axisymmetric geometry. For the further study, Afkhami et al. [16] reported the experimental data on the deformation of a biocompatible ferrofluid droplet suspended in a viscous medium under uniform magnetic fields, and the result showed the droplet elongating along the direction of the magnetic field direction. Also, they used the same numerical approaches to study this problem. At low magnetic fields, the final droplets achieved in simulations showed excellent agreement with their experiments in the shape as well as the aspect ratio. At high magnetic fields, however, the droplet elongation was overpredicted by the simulations.

Using VOSET method, Shi et al. [17] performed a 2D numerical simulation on ferrofluid droplet falling in a nonmagnetic fluid when exposed to a uniform magnetic force. The effects of the magnetic Bond number, susceptibility, Weber number, Reynolds number, and magnetic field direction on the motion and deformation of droplet were investigated systematically. The results indicated that an increase in magnetic Bond number or susceptibility leads to larger degree of the droplet deformation.

Ghaffari et al. [18] simulated the deformation of ferrofluid droplet subjected to uniform magnetic field and investigated some parameters influencing the droplet shape at equilibrium including the magnetic field intensity, droplet size, and surface tension. The simulations were conducted on CFD package OpenFOAM with CLSVOF method applied for the interface capturing. From the data collected in their simulations, a correlation was proposed for the prediction of the aspect ratio at equilibrium.

Capobianchi et al. [19] performed a two-dimensional investigation on the dynamics of a ferrofluid in a shear flow subjected to a uniform magnetic field. The result suggests the droplet deformation and inclination angle varies with the applied magnetic field intensity.

Liu et al. [20] carried out experimental and numerical studies on the process of ferrofluid droplet formation, and a uniform magnetic field was applied parallel with the flow direction. In the presence of the magnetic field, the result suggests longer formation time and greater size of the formed droplet for the additional magnetic takes a pulling effect on the droplet tip. Liu et al. [21] employed a particle Level-set method on the simulation of this problem and obtained similar results.

Using VOF for the interface tracking, Sen et al. [22] numerically studied ferrofluid droplet generation in a T-junction considering a magnetic field produced by two external magnetic dipoles. The influences by parameters including dipole location, surface tension on the droplet formation period and the formed droplet size were investigated. A simplification was used in their study that the ferrofluid does not alter the magnetic field applied. Aboutalebi et al. [23] conducted a numerical investigation on the splitting process of ferrofluid droplet in a T-shaped junction. Under an asymmetric magnetic field applied, the splitting at the junction resulted in unequal sizes of the daughter droplets.

Varma et al. [24] performed numerical and experimental studies on the generation of ferrofluid droplets under the influence of a uniform magnetic field. The result suggests that droplet size, shape, and interdroplet spacing can be controlled by turning the magnetic permeability, the viscosity, and the flow rate of the nonmagnetic fluid. On this basis, Ray et al. [25] studied the dynamics of merging between two ferrofluid droplets as well as between a ferrofluid droplet and a nonmagnetic one.

The deformation and orientation of a ferrofluid droplet in a simple shear flow in presence of a uniform magnetic field focused in an arbitrary direction were investigated numerically by Hassan et al. [26]. In their studies, the conservative Level-set method was applied to track the evolution of interface. The effects of the magnetic field on the deformation and orientation of the ferrofluid droplet by varying the magnetic field direction, magnetic bond number, and capillary number were studied in detail. In addition, a versatile method for controlling the lateral migration of ferrofluid droplets by adjusting the magnetic field direction was demonstrated by combining the wall-bound simple shear flows and uniform magnetic fields.

A robust two-dimensional hybrid lattice-Boltzmann/finite-volume method coupled magnetic field equations was developed by Ghaderi et al. [27] and the falling ferrofluid droplet behavior in nonmagnetic fluid under a uniform field was performed by a set of numerical simulations. Two cases including the falling droplet and the deformation of static drop were considered to validate the proposed method. Furthermore, the effects of the magnetic field including magnetic Bond number, susceptibility and magnetic field direction on the deformation of the falling droplet were discussed, and the results were consistent with those reported by Shi et al. [17].

As can be seen, the existing numerical studies are mostly focused on the behaviors of ferrofluid droplet in uniform magnetic fields, and little research has been devoted to nonuniform magnetic field. In many applications, however, nonuniform and varying magnetic fields are required for the manipulations on ferrofluid droplets. The mechanism of the motion and deformation of ferrofluid droplet under nonuniform magnetic field are rather different from those in uniform field. In the present study, we performed a three dimensional numerical simulation to investigate the behaviors of a ferrofluid droplet in nonuniform magnetic field and to study how the magnetic force influence the motion of the droplet. The rest of the present article is organized as follows. The problem studied is described in [Section 2](#). In [Section 3](#), we present the numerical approaches applied in the present study. The results are illustrated and discussed in [Section 4](#). Some limitations of this study and its possible extensions are discussed in [Section 5](#). Finally, some conclusions are made in [Section 6](#).

2. Problem description and computational setup

[Figure 1](#) sketches the problem studied. We consider a vertical rectangular tube with a circular wire loop coaxially placed around it. The tube is filled with a nonmagnetic fluid and a ferrofluid droplet, and they are respectively considered as the continuum and the dispersed phases in the present study. The nonuniform magnetic field is produced by a steady electric current passing through the wire loop. The ferrofluid droplet is initially positioned at the tube center with a certain distance below the wire loop, and it moves under the effects of gravity as well as the produced magnetic force.

In the present study, the discretized domain for the rectangular channel is 8 mm in length and 5 mm in width. Periodic conditions were specified on the top and the bottom boundaries, and no-slip wall conditions were set on the other four boundaries. The wire loop has a radius of 5 mm, and is located at the central height of the tube, namely, $z = 4$ mm. The initial ferrofluid droplet having a radius of 1 mm is centered 2 mm below the wire loop. As for the physical properties of the two phases, we followed the biocompatible ferrofluid reported by Afkhami et al. [16] as the dispersed phase, which is composed of Fe_3O_4 nanoparticles with a mean diameter of

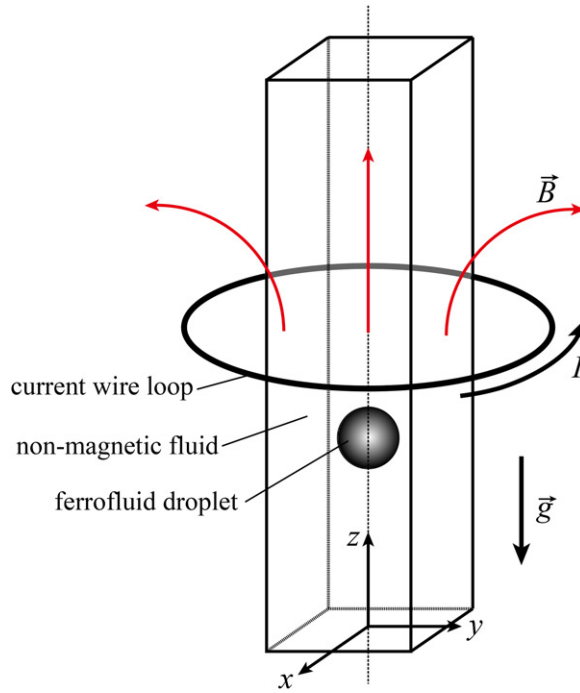


Figure 1. Illustration of the problem studied: a ferrofluid droplet moves under a nonuniform magnetic field produced by an electric current loop.

Table 1. Physical properties of the continuum and the dispersed phases

| Phase | Density (kg/m^3) | Viscosity (N·s/m) | Magnetic permeability | Surface tension (N/m) |
|-----------|-----------------------------|-------------------|-----------------------|-----------------------|
| Continuum | 1000 | 0.01 | μ_0 | – |
| Dispersed | 1260 | 0.001 | $1.8903\mu_0$ | 0.0135 |

7.2 nm, and set water as the continuum phase. The physical properties of the two phases are summarized in Table 1, in which $\mu_0 = 4\pi \times 10^{-7} \text{ N/A}^2$ is the magnetic permeability of vacuum. Additionally, the gravity acceleration was specified as 9.8 m/s^2 .

3. Numerical methods

3.1. Interface tracking method

The ferrofluid droplet dynamics subjected to magnetic field can be considered as a kind of incompressible free surface flow with interaction between a magnetic phase and a nonmagnetic one. An important problem in simulating free surface flow is the capture of the phase boundary. Sun et al. [28] proposed a VOSET method which combines the advantages and overcomes the disadvantages of Volume-of-Fluid and Level-set methods for capturing interface. In our previous paper [29], we developed a three-dimension VOSET method in which new approaches were used to deal with new geometric problems. In this study, the 3D VOSET method was applied to capture the interface of ferrofluid droplet. The volume fraction (denoted by f), which represents the volume proportion of the ferrofluid phase in a computational cell, is calculated by its governing equation:

$$\frac{\partial f}{\partial t} + \mathbf{u} \cdot \nabla f = 0 \quad (1)$$

At each time step, a level-set function, denoted by ϕ , is geometrically generated from the reconstructed interfaces in VOF for the purpose of more accurate calculations of interface normal and curvature. A smoothed Heaviside function varying from 0 to 1 is applied for the numerical smearing of surface tension and magnetic forces, and it is calculated by the level-set function:

$$H(\phi) = \begin{cases} 0 & \phi < -\varepsilon \\ \frac{1}{2} \left(1 + \frac{\phi}{\varepsilon} + \frac{1}{\pi} \sin \frac{\pi\phi}{\varepsilon} \right) & -\varepsilon \leq \phi \leq \varepsilon \\ 1 & \phi > \varepsilon \end{cases} \quad (2)$$

in which ε is an adjustable parameter specified as 1.5Δ (Δ denotes the grid size). Simultaneously, its derivative, namely smoothed delta function, is given by the following.

$$\delta(\phi) = \begin{cases} 0 & |\phi| > \varepsilon \\ \frac{1}{2\varepsilon} \left(1 + \cos \frac{\pi\phi}{\varepsilon} \right) & |\phi| \leq \varepsilon \end{cases} \quad (3)$$

3.2. Governing equation of magnetic field

For nonconducting ferrofluid considered in the present study, the Maxwell equations can be simplified as equations for magnetic induction \mathbf{B} , magnetic field \mathbf{H} , and magnetization \mathbf{M} :

$$\nabla \cdot \mathbf{B} = 0 \quad (4)$$

$$\nabla \times \mathbf{H} = 0 \quad (5)$$

$$\mathbf{B} = \mu_0(\mathbf{H} + \mathbf{M}) \quad (6)$$

In the nonmagnetic phase, the magnetization vanishes. Using a linear magnetization assumption for the ferrofluid, the magnetization satisfies $\mathbf{M} = \chi\mathbf{H}$, in which χ is the magnetic susceptibility. Therefore, Eq. (6) can be simplified as:

$$\mathbf{B} = \mu\mathbf{H} \quad (7)$$

in which $\mu = (1 + \chi)\mu_0$ takes different values in the two phases.

Thanks to the irrotational feature of the magnetic field (Eq. (5)), one can introduce a magnetic scalar potential ψ such that

$$\mathbf{H} = -\nabla\psi \quad (8)$$

Associating Eqs. (7) and (8), Eq. (4) can be then converted into a governing equation of the magnetic scalar potential for nonconducting medium:

$$\nabla \cdot (\mu\nabla\psi) = 0 \quad (9)$$

3.3. Governing equation for fluid flow

The *one-fluid* formulation [30] is used to describe the incompressible two-phase flow. Considering the influences by gravity, surface tension, and magnetic force, the continuity equation and momentum equation can be written as:

$$\nabla \cdot \mathbf{u} = 0 \quad (10)$$

$$\frac{\partial(\rho\mathbf{u})}{\partial t} + \nabla \cdot (\rho\mathbf{u} \otimes \mathbf{u}) = -\nabla p + \nabla \cdot (\eta\nabla\mathbf{u} + \eta\nabla\mathbf{u}^T) + \rho\mathbf{g} + \mathbf{F}_\sigma + \mathbf{F}_H \quad (11)$$

The physical properties appearing in the governing equations, which include density, viscosity, and magnetic permeability, are calculated by the smoothed Heaviside function. Concretely,

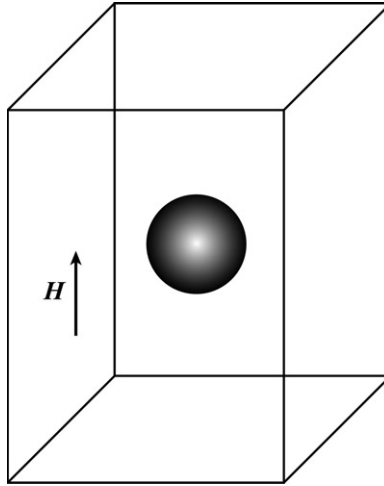


Figure 2. Validation problem: a spherical ferrofluid droplet deforms in a uniform magnetic field (corresponding experiments were carried out by Afkhami et al. [16]).

$$\begin{aligned}
 \rho &= H(\phi)\rho_d + (1 - H(\phi))\rho_c \\
 \eta &= H(\phi)\eta_d + (1 - H(\phi))\eta_c \\
 \mu &= H(\phi)\mu_d + (1 - H(\phi))\mu_c
 \end{aligned} \tag{12}$$

In this way, these properties take their individual values in the continuum and dispersed phases, and vary smoothly across the phase boundary.

In Eq. (11), F_σ and F_H respectively denote the surface tension force and the magnetic force, which are diffused in a narrow region around the phase boundary. The surface tension is discretized into volume force by CSF model [31] expressed as:

$$F_\sigma = \sigma\kappa\delta(\phi)\mathbf{n} \tag{13}$$

For a linearly magnetizable medium the magnetic force can be transformed into surface force on the phase boundary, and then be smeared by the smoothed delta function [17, 32]:

$$F_H = \frac{1}{2}|\mathbf{H}|^2(\mu_d - \mu_c)\delta(\phi)\mathbf{n} \tag{14}$$

Regarding the schemes and algorithms for solving Navier-Stokes equation, one can refer to Ref. [29] for the details.

4. Numerical results

4.1. Validation: droplet deformation in uniform magnetic field

The employed three-dimensional interface tracking method, VOSET, have been assessed by the present authors [29] in terms of simulating liquid-gas multiphase. To validate its accuracy in simulating free surface flow of ferrofluid under the effect of magnetic field, we first carried out a numerical test on a droplet deformation in uniform magnetic field. As shown in Figure 2, the ferrofluid droplet was placed at the center of a computational domain with uniform magnetic field specified in the vertical direction. Following the experiments reported by Afkhami et al. [16], the ferrofluid droplet in the validation problem was specified as 1.291 mm, and gravity was not taken into consideration. The magnetic field intensity was varied from 2 kA/m to 7 kA/m.

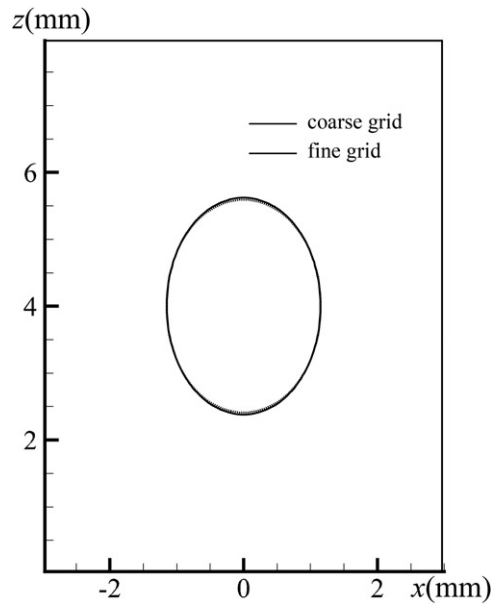


Figure 3. Final interface locations at $H = 7$ kA/m on the x - O - z cross section achieved under two grid resolutions.

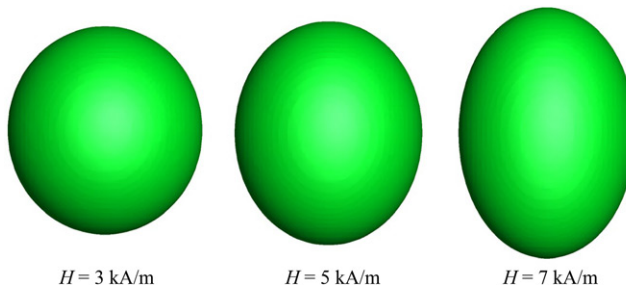


Figure 4. Droplet shapes at equilibrium.

At first, we used a coarse mesh and a fine one having grid sizes of $\Delta = 0.125$ mm and $\Delta = 0.0625$ mm, respectively, to simulate the droplet deformation at the magnetic field intensity of 7 kA/m. **Figure 3** compares the phase boundaries at the x - O - z central cross section when equilibrium was reached. It clearly shows the droplet elongation along the direction of the applied uniform magnetic field, and more importantly, the interface locations obtained in the two grids are almost coincident. Therefore the two grid sizes are fine enough for the ferrofluid droplet motions in the present study. We used the finer grid size with $\Delta = 0.0625$ mm for the rest simulations.

Figure 4 displays the droplet at equilibrium at $H = 3$ kA/m, $H = 5$ kA/m, and $H = 7$ kA/m. It elongates along the magnetic field direction (z -direction) and finally reaches a specific aspect ratio which can be regarded as a measurement of the droplet deformation. The aspect ratio at equilibrium under various magnetic field intensities are plotted in **Figure 5**, in which the experimental measurements by Afkhami et al. [16] are included for comparison. One can see that the numerical results of b/a of the elongated sphere (for the simplicity aspect ratio) predicted by our numerical model confirm fairly well with experiments. The excellent agreement in the present section confirms that the numerical methods introduced in **Section 3** can be applied in studying the dynamic behaviors of ferrofluid droplet exposed in external magnetic field.

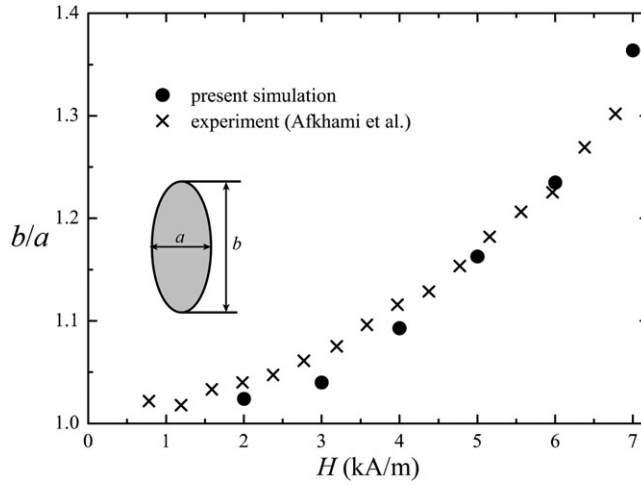


Figure 5. A comparison between final aspect ratios by numerical simulation and experiments (Afkhani et al. [16]).

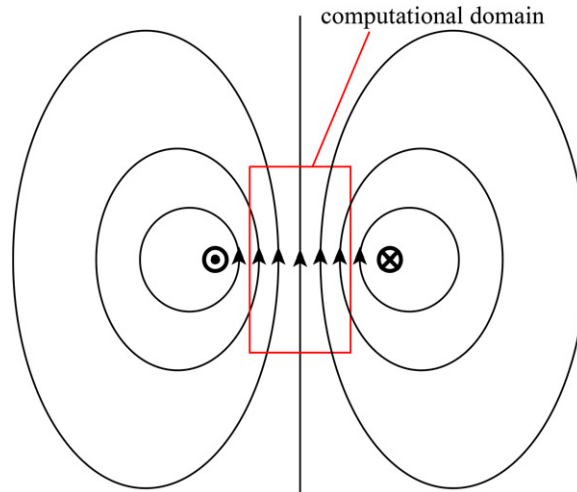


Figure 6. Computational domain used in solving the magnetic field.

4.2. Magnetic field generated by a circular wire loop

According to Biot-Savart law, the produced magnetic field at any location can be calculated by the integration over the wire loop.

$$\mathbf{H}(\mathbf{r}) = \frac{1}{4\pi} \oint_{loop} \frac{Id\mathbf{l} \times \mathbf{r}'}{|\mathbf{r}'|^2} \quad (15)$$

In the present study, the magnetic scalar potential as well as the magnetic field are solved in a finite domain (see Figure 6), and therefore boundary conditions need to be given on its borders. When solving the magnetic potential ψ (Eq. (9)), Neumann conditions are specified on all boundaries. For a specific cell face on boundary (denoted by b), the normal gradient of the magnetic scalar potential can be calculated based on Eq. (8):

$$\left(\frac{\partial \psi}{\partial n} \right)_b = \mathbf{n}_b \cdot (\nabla \psi)_b = -\mathbf{n}_b \cdot \mathbf{H}_b \quad (16)$$

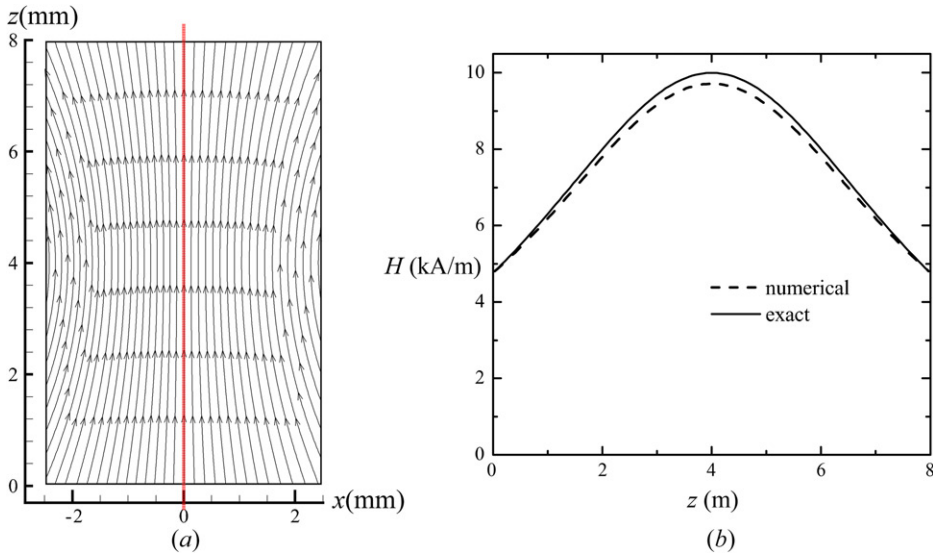


Figure 7. Nonuniform magnetic field produced by a circular wire loop: (a) Magnetic field lines; (b) Magnetic field intensity along the axis line.

in which \mathbf{n}_b refers to the unit normal the cell face, and \mathbf{H}_b is calculated directly by Bio-Savart law (Eq. (15)).

A test problem was studied to assess the numerical approaches (Eq. (16)) in mimicking the nonuniform magnetic field produce by the electric current loop in a finite region. Assuming the entire computational domain was filled with the nonmagnetic phase, we solved the magnetic scalar potential by its governing equation (Eq. (9)) and its Neumann boundary conditions (Eq. (16)) at electric current intensity of $I = 100$ A. The magnetic field H was then calculated by Eq. (8).

Figure 7a illustrates the obtained magnetic field line on the x - O - z cross section. Note, the wire loop is located at $z = 4$ mm. It clearly shows a nonuniform magnetic field and a similar feature to the local magnetic field at the internal region of a circular electric current loop. In this problem, the exact magnetic field intensity along the axis of the wire loop is given as:

$$H = \frac{1}{2} \frac{a^2 I}{(a^2 + \Delta z^2)^{3/2}} \quad (17)$$

Figure 7b plots the numerically obtained magnetic field intensity as well as the one by Eq. (17), which show excellent consistency. The largest deviation occurring at the loop center is lower than 3%.

Figure 8a shows the magnetic field lines on the x - O - z cross section with the ferrofluid droplet placed at the center of the wire loop. It can be seen that, owing to the magnetization, the droplet distorted the magnetic field lines at its local. Since the magnetic field on the boundaries are given as the one without magnetic medium, the computational domain in the transverse directions (x - and y -directions) needs to be wide enough such that the side boundaries do not overlap with the affected zone by the ferrofluid droplet. We conducted the same calculations under different widths of the computational domain to evaluate the boundary effect in terms of solving the magnetic field. Figure 8b plots four magnetic field intensities along a horizontal line passing through the droplet center (see the red dash line in Figure 8a) under widths of 3 mm, 4 mm, 5 mm, and 6 mm, respectively. Also, the magnetic field intensity without ferrofluid droplet is plotted as the black solid line. By comparison, we consider that the magnetic field intensity solved under the width of 5 mm gives acceptable deviation (less than 3%) at the side boundaries.

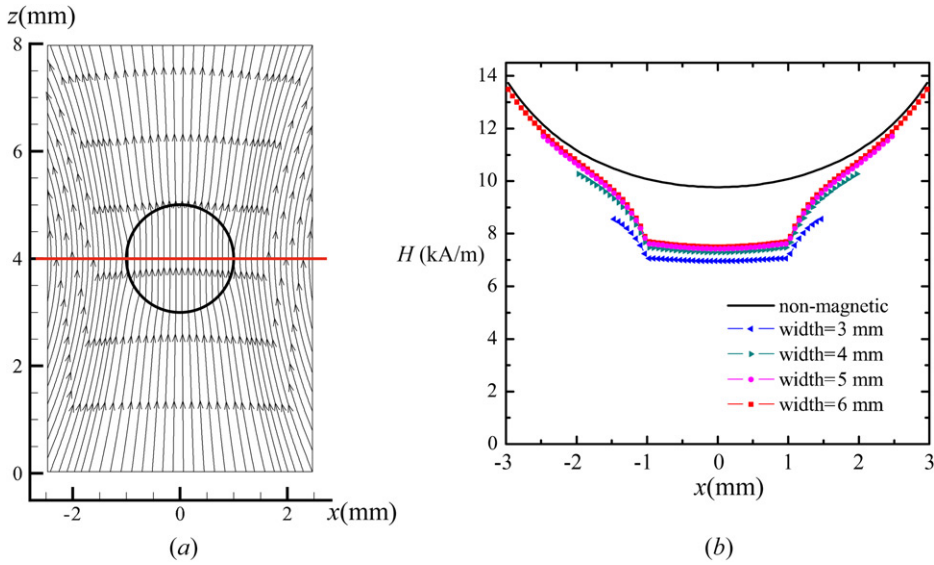


Figure 8. Magnetic field around a spherical ferrofluid droplet: (a) Magnetic field lines on the x-O-z cross section; (b) Magnetic field intensity along the horizontal central line obtained under different widths of the computational domain.

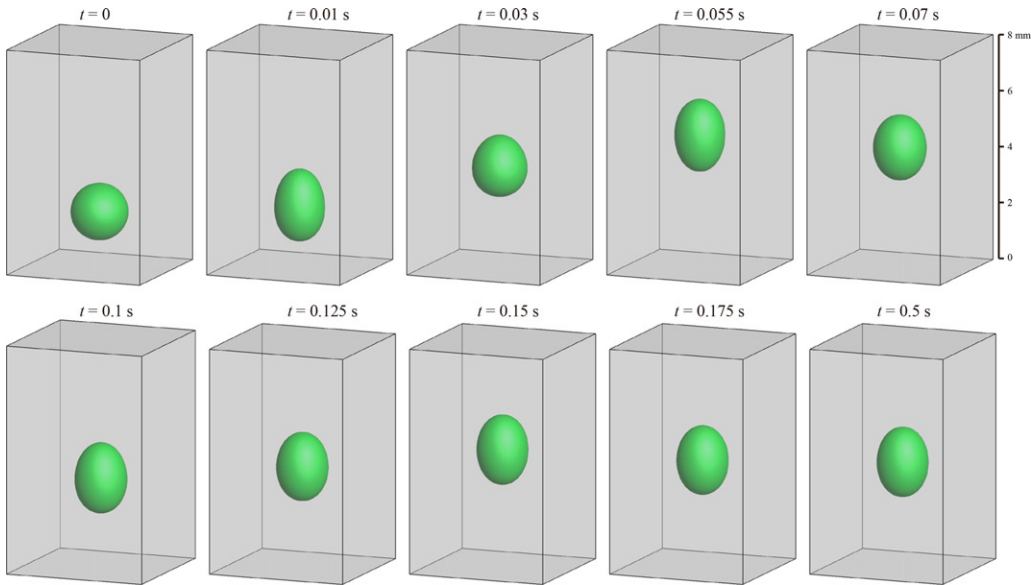


Figure 9. Interface evolution of the case with $I = 100$ A.

4.3. Dynamics of droplet motion and deformation

After the validations, attention is now turned to the problem described in Figure 1. For the first case we set the electric current intensity in the wire loop (see Figure 1) as $I = 100$ A, which corresponds to a magnetic field intensity of 10 kA/m at its center. The ferrofluid droplet was initially placed with at a certain distance below wire loop. Using the numerical methods introduced in Section 3, the dynamics of the droplet motion under the effects of magnetic force, surface tension and gravity was simulated until $t = 0.5$ s.

In the absence of magnetic field, the droplet will settle owing to its greater density than the continuum phase, but its motion may proceed in a different manner with a nonuniform magnetic field applied. Figure 9 illustrates the droplet motion as well as deformation during in the

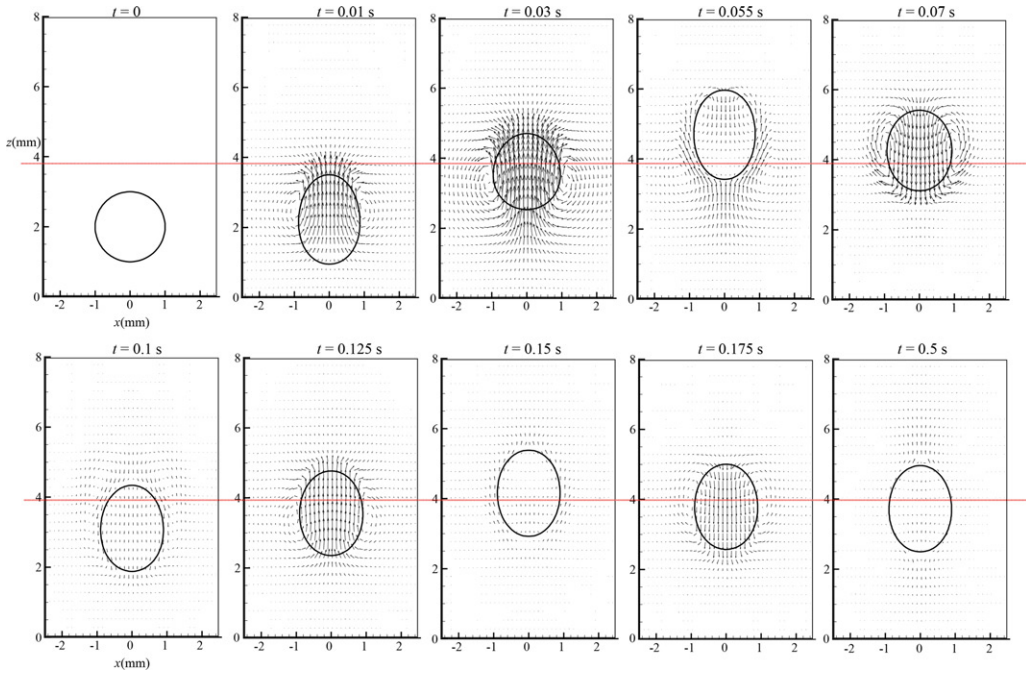


Figure 10. Flow fields at different instances on the x - O - z cross section.

nonuniform magnetic force produced by the circular wire loop. The ferrofluid droplet oscillates along the axis until reaching equilibrium status. Correspondingly, the velocity vectors on the central cross section (x - O - z plane) are displayed in [Figure 10](#), in which the red dash lines indicate the location of the wire loop.

Regarding its deformation, the ferrofluid droplet almost reached a fixed aspect ratio at $t = 0.15$ s and kept its shape unchanged thereafter. In a short span, the initial spherical droplet elongated in the vertical direction, reaching an ellipsoidal shape. From the velocity field at $t = 0.01$ s, we can see the droplet globally moved upwards, which indicates the net magnetic force applied on droplet was in the upward direction and its magnitude was great enough to overcome the gravity. Such magnetic force lies in the nonuniform magnetic field applied. As can be seen in [Figure 7b](#), the magnetic field intensity increases with the vertical location when $z < 4$ mm, and therefore, the initial droplet placed below the wire loop has stronger magnetic field at its upper half than at its lower half.

The droplet continued rising with its center getting across the wire loop at around 0.03 s. After that the net magnetic force was in the downward direction since the magnetic field intensity was greater at the lower half of the droplet. The droplet began to fall after reaching a maximum height at around $z = 6$ mm. Under the applied nonuniform magnetic field, the droplet continued oscillating. In order to monitor the droplet motion, the location of the droplet volume center, calculated as

$$h_d = \frac{\int_{\Omega} fz dV}{\int_{\Omega} f dV} \tag{18}$$

is plotted as the solid line in [Figure 11](#). As it can be seen that, the droplet moved up and down around a certain location with a period of about 0.1 s. Meanwhile, the amplitude kept decreasing

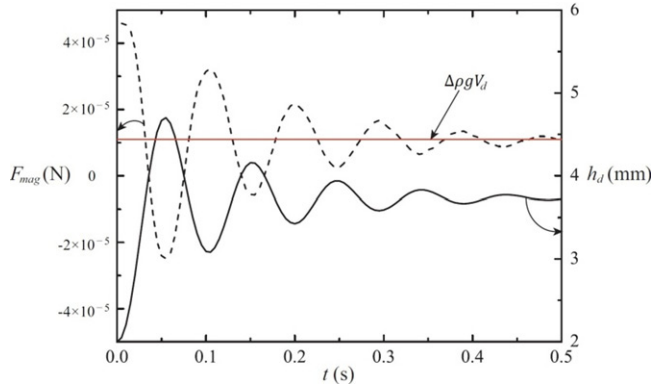


Figure 11. Droplet volume center location and the net magnetic force imposed on the droplet.

due to the damping effect of the continuum phase. The net magnetic force in the vertical direction, calculated as

$$F_{mag} = \int_{\Omega} F_H \cdot e_z dV \quad (19)$$

is plotted as the dash line in [Figure 11](#). The positive and negative values of F_{mag} respectively correspond to upward and downward magnetic force imposed on the ferrofluid droplet. [Figure 11](#) shows that the magnetic force oscillates with the droplet motion. Though a careful observation, one can find that the net magnetic force is positive as the droplet center is located below the wire loop ($h_d < 4$ mm), and vice versa. As the droplet finally rests and stays in a fixed location, the magnetic force and the gravity force should reach equilibrium. The value of the gravity force is plotted as the red line in [Figure 11](#), which can be simply calculated as $(\rho_d - \rho_c)gV_d = 1.1 \times 10^{-5}$ N. It shows that, during the droplet oscillation, the net magnetic force is getting close to the gravity force in magnitude, which suggests that the droplet is approaching equilibrium status.

4.4. Influences of the current intensity

To evaluate the influence of the nonuniform magnetic field intensity on the droplet motion, we next varied the electric current intensity from 40 A to 120 A while keeping other parameters unchanged. The droplet center locations versus time under those conditions are plotted in [Figure 12](#). From the green line, we can see that when $I = 40$ A, the ferrofluid droplet starts to settle at the beginning, which indicates that the magnetic field produced at such electric current intensity cannot provide the droplet with enough lifting force to overcome the gravity at its initial location.

As for the other cases with stronger current electric current intensity, the droplet initially rose and then kept oscillating until it stayed at a specific location below the wire loop. It suggests a critical electric current intensity between 40 A and 60 A for the wire loop to prevent the ferrofluid droplet from settling. The net magnetic force imposed on the droplet at its initial location (2 mm below the wire loop) calculated by [Eq. \(19\)](#) under various electric current intensity is plotted as [Figure 13](#). By comparing with the gravity force, one can find that the critical electric current intensity is around 49 A.

In the cases with $I = 60 \sim 120$ A, the ferrofluid droplet oscillated around the wire loop. It should be noted that, for the current intensities of 60 A and 80 A we found that the droplet motion is far from reaching equilibrium at $t = 0.5$ s, and therefore another 0.25 s was extended for the two cases. By comparison among those cases we can find that, first, the droplet oscillates at

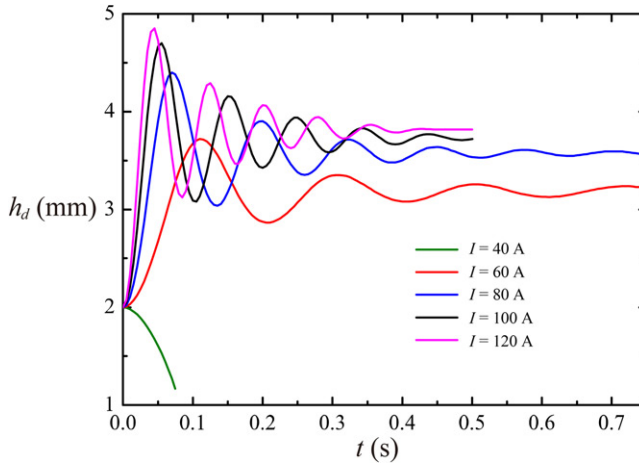


Figure 12. Droplet motions under different intensities of electric current.

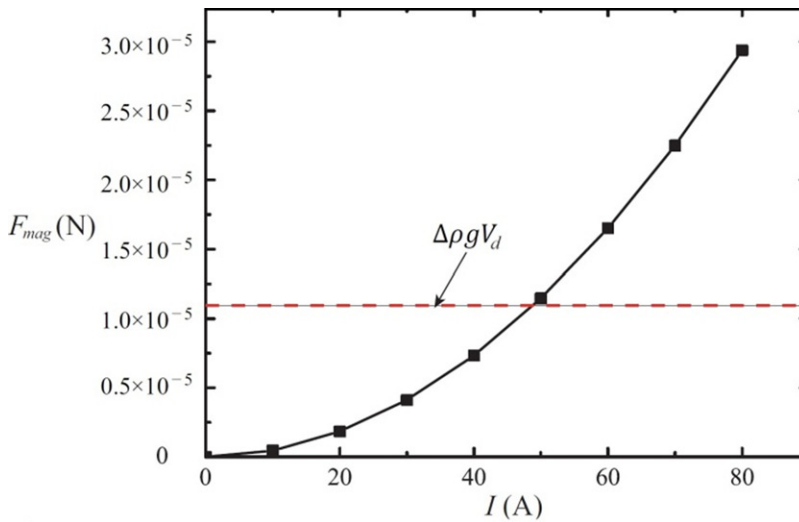


Figure 13. Net magnetic force provided by the wire loop with various intensities of electric current.

higher frequency in greater intensity of the electric current. It lies in the stronger response resulting from the stronger magnetic field in pulling the droplet back to its equilibrium location. Second, in all those cases the droplet finally rests below the wire loop ($z = 4$ mm), and stronger electric current leads to a closer distance from the drop center to the wire loop. Indeed, for all those cases, the same magnitude of the magnetic force was applied on the droplet at equilibrium status. Figure 14 illustrates the phase boundaries as simulations terminated when equilibrium status is almost reached. It confirms a closer distance to the wire loop at a stronger magnetic field. Meanwhile, we can find a larger degree of elongation of the droplet in a stronger magnetic field than in a weaker one. Specifically, the smallest current intensity ($I = 60$ A) and the largest one ($I = 120$ A) result in aspect ratios of 1.13 and 1.56, respectively.

4.5. Magnetic force imposed on spherical droplet

We have found that the magnetic force plays an important role in pulling the ferrofluid droplet to the central location of the wire loop, and the intensity of the force varies with the droplet

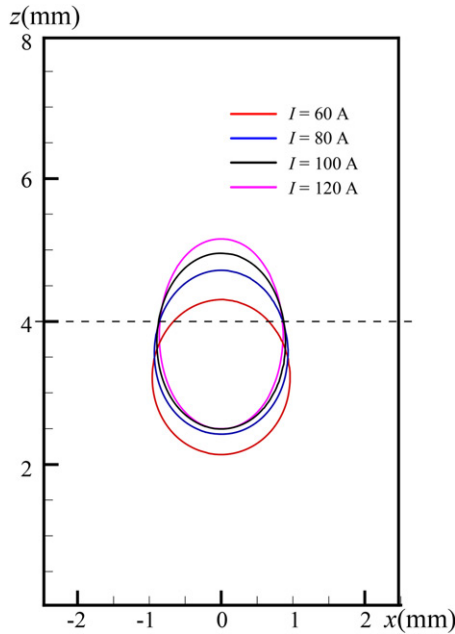


Figure 14. Final droplet shapes and locations under different intensities of electric current.

location as well as the electric current intensity. To give a quantitative insight into the effect of the wire loop, we have carried out a set of numerical calculations for the net magnetic force imposed on the ferrofluid droplet under various locations and electric current intensities. Note, in the calculations presented in this section the droplet is spherical.

Figure 15 displays the net magnetic force imposed on the droplet under various electric current intensity and distances to the wire loop. From any curve on this figure one can find that, as the droplet moves progressively away from the wire loop center, the magnetic force initially increases. It lies in the increasing asymmetry of the magnetic field around the droplet. However, as the droplet continues moving away from the wire loop, the magnetic field around gets progressively weaker, and the produced magnetic force approaches zero. The peak value is reached at a distance of around 2 mm regardless of the current intensity. At any specific location, obviously, the magnitude of the magnetic force increases with the current intensity.

From the data (Figure 15) achieved numerically, a correlation for the net magnetic force (in Newtons) of a spherical droplet locating on the axis was fitted using a least square approach:

$$F_{mag} = 2.26 \times 10^{-4} \left(\frac{\Delta z}{a} \right)^{1.07} \left[1 + \left(\frac{\Delta z}{a} \right)^2 \right]^{-4.04} \left(\frac{I}{I_{ref}} \right)^2 \quad (20)$$

In Eq. (20) a ($= 5$ mm) is the radius of the wire loop, and I_{ref} ($= 100$ A) is the reference current intensity.

Figure 16 compares the magnetic forces obtained by our simulations and those predicted by Eq. (20). The average and the largest discrepancies between them are 0.26% and 7.2%, respectively. It suggests the proposed correlation (Eq. (20)) has excellent accuracy in repeating the characteristics of the magnetic force imposed on a spherical droplet.

The numerical data as well as the correlation presented in this section are based on spherical droplet without considering its deformation. To evaluate how well Eq. (20) describes the magnetic force on the droplet with deformation. We compared the magnetic forces by simulations and by predictions in two cases with $I = 60$ A and $I = 120$ A, and the results are plotted in Figure 17. The

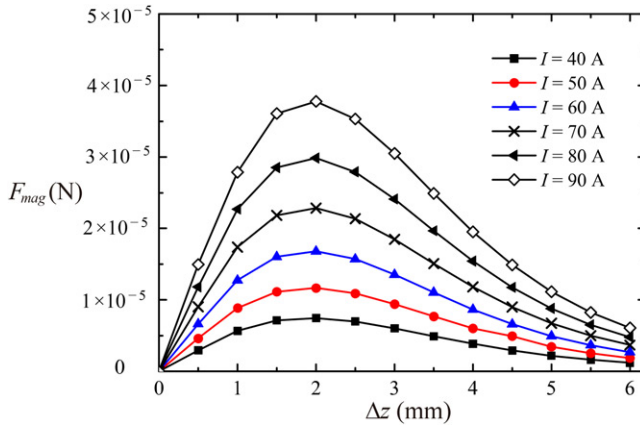


Figure 15. Net magnetic force imposed on the spherical ferrofluid droplet under different electric current intensities and distances to the wire loop.

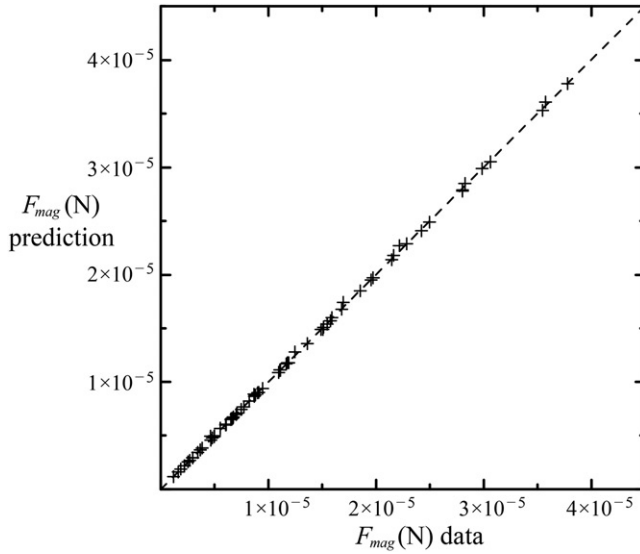


Figure 16. Comparison between magnetic forces achieved by numerical calculations and the proposed correlation (Eq. (20)).

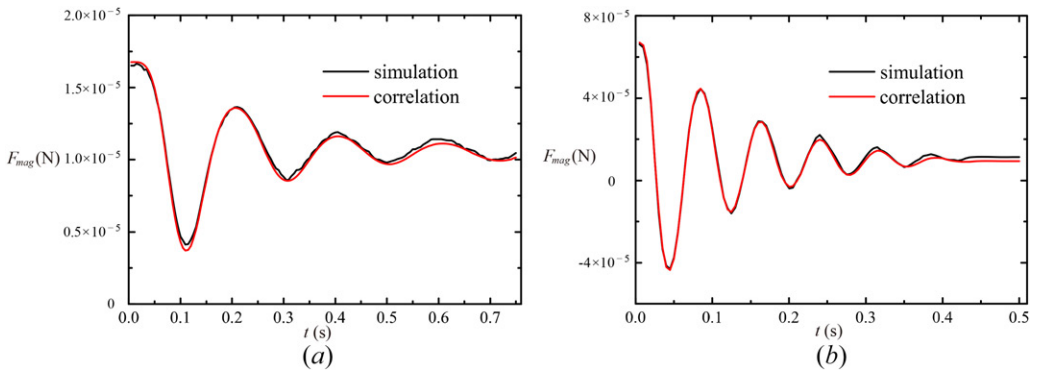


Figure 17. Comparison between the net magnetic force imposed on the ferrofluid droplet by our simulation and the one by the proposed correlation for: (a) $I = 60$ A; (b) $I = 120$ A.

black solid line represents the magnetic force calculated by Eq. (19) considering the droplet deformation, and the red line denotes the predicted force using the proposed correlation (Eq. (20)), in which the droplet location was calculated by Eq. (18). From both cases we can find, in spite of droplet deformations, the proposed correlation can give a general prediction on the net magnetic force in the two cases with acceptable accuracy. Even in the case with $I=120$ A, where the ferrofluid droplet shape deviates most from spherical, the correlation predicts the magnetic force fairly well. It also indicates that the magnetic force on the ferrofluid droplet is not much affected by the degree of droplet deformation.

5. Limitations of the present study

Finally, we would like to discuss on some limitations of the present study. First, in our numerical framework the magnetic field and the flow field were solved in the same computational domain. In many applications of ferrofluid [4, 6, 22, 23], the droplet and its surrounding fluid flow in a limited region such as a narrow tube in a lab-on-chip device, while the magnetic field is usually produced outside and needs to be considered in a larger region. As the droplet approaches the wall boundary, its distortion effect on the magnetic field line outside the flow region is no longer negligible. A numerical framework with multiple regions which allows the magnetic field be solved in an extended computational domain may provide as a solution for this issue.

Second, although the proposed correlation (Eq. (20)) only applies for the magnetic forces on ferrofluid droplets located on the central axis of a current wire loop, its validations suggests it is possible to build up a model which gives a satisfying accuracy for magnetic force imposed on ferrofluid droplets within a certain degree of its deformation. In real applications, droplets are usually exposed in more complicated nonuniform magnetic fields than the one considered in the present study. The prediction of magnetic force may therefore require more sophisticated models which can take account of other parameters, such as droplet aspect ratio and magnetic permeability.

6. Conclusions

A three-dimensional numerical investigation has been carried out upon the dynamics of ferrofluid droplet exposed in nonuniform magnetic field produced by an electric current loop. A coupled volume-of-fluid and level-set interface tracking method, VOSET, was used for handling the moving boundary.

A validation problem in which a ferrofluid deforms in uniform magnetic field was first studied, and the obtained aspect ratios confirm closely with reported experimental data. The investigations regarding nonuniform magnetic field revealed many features in the dynamics of the ferrofluid droplet. The electric wire loop gives an attractive effect upon the ferrofluid droplet through the nonuniform magnetic field it produces. When the magnetic force is great enough to overcome the gravity, the ferrofluid droplet oscillates around the wire loop, and finally it rests and reaches an equilibrium location under the damping effect of the continuum phase. As the current and the produced magnetic field intensity increases, the ferrofluid droplet oscillates at a higher frequency and finally reaches a larger degree of deformation.

A set of numerical simulations were conducted for the net magnetic force on spherical ferrofluid droplet at various locations on the central axis of the wire loop. The magnetic force initially increases and then decreases as the droplet progressively moves away from the wire loop. From the data achieved, a correlation was build up, and it gives accurate prediction in the magnitude of the magnetic force on the droplet within a certain degree of droplet deformation.

Funding

This work has been supported by China Postdoctoral Science Foundation (2018M6333506) and the Foundation for Innovative Research Groups of the National Natural Science Foundation of China (No. 51721004).

References

- [1] R. Rosensweig, *Ferrohydrodynamics*. Cambridge: Cambridge University Press, 1985.
- [2] M. Cowley and R. Rosensweig, "The interfacial stability of a ferromagnetic fluid," *J. Fluid Mech.*, vol. 30, no. 04, pp. 671–688, 1967. DOI: [10.1017/S0022112067001697](https://doi.org/10.1017/S0022112067001697).
- [3] A. Dickstein, S. Erramilli, R. Goldstein, D. Jackson, and S. A. Langer, "Labyrinthine pattern formation in magnetic fluids," *Science*, vol. 261, no. 5124, pp. 1012–1015, 1993. DOI: [10.1126/science.261.5124.1012](https://doi.org/10.1126/science.261.5124.1012).
- [4] Y. Sun, Y. Kwok, and N. Nguyen, "A circular ferrofluid driven microchip for rapid polymerase chain reaction," *Lab Chip*, vol. 7, no. 8, pp. 1012–1017, 2007. DOI: [10.1039/b700575j](https://doi.org/10.1039/b700575j).
- [5] H. Hartshorne, C. Backhouse, and W. Lee, "Ferrofluid-based microchip pump and valve," *Sens. Actuators B Chem.*, vol. 99, no. 2-3, pp. 592–600, 2004. DOI: [10.1016/j.snb.2004.01.016](https://doi.org/10.1016/j.snb.2004.01.016).
- [6] Y. Chang, C. Hu, and C. Lin, "A microchannel immunoassay chip with ferrofluid actuation to enhance the biochemical reaction," *Sens. Actuators B Chem.*, vol. 182, pp. 584–591, 2013. DOI: [10.1016/j.snb.2013.03.078](https://doi.org/10.1016/j.snb.2013.03.078).
- [7] K. Raj and R. Moskowitz, "Commercial applications of ferrofluids," *J. Magn. Magn. Mater.*, vol. 85, no. 1-3, pp. 233–245, 1990. DOI: [10.1016/0304-8853\(90\)90058-X](https://doi.org/10.1016/0304-8853(90)90058-X).
- [8] Z. Wang, R. Wu, Z. Wang, and R. Ramanujan, "Magnetic trapping of bacteria at low magnetic fields," *Sci. Rep.*, vol. 6, pp. 26945, 2016. DOI: [10.1038/srep26945](https://doi.org/10.1038/srep26945).
- [9] Q. Liu, S. Alazemi, M. Daqaq, and G. Li, "A ferrofluid based energy harvester: Computational modeling, analysis, and experimental validation," *J. Magn. Magn. Mater.*, vol. 449, pp. 105–118, 2018. DOI: [10.1016/j.jmmm.2017.09.064](https://doi.org/10.1016/j.jmmm.2017.09.064).
- [10] X. Liu *et al.*, "Preparation and characterization of biodegradable magnetic carriers by single emulsion-solvent evaporation," *J. Magn. Magn. Mater.*, vol. 311, no. 1, pp. 84–87, 2007. DOI: [10.1016/j.jmmm.2006.10.1170](https://doi.org/10.1016/j.jmmm.2006.10.1170).
- [11] O. Mefford *et al.*, "Field-induced motion of ferrofluids through immiscible viscous media," *J. Magn. Magn. Mater.*, vol. 311, no. 1, pp. 347–353, 2007. DOI: [10.1016/j.jmmm.2006.10.1174](https://doi.org/10.1016/j.jmmm.2006.10.1174).
- [12] M. Korlie, A. Mukherjee, B. Nita, J. Stevens, A. Trubatch, and P. Yecko, "A ferrofluid based energy harvester: Computational modeling, analysis, and experimental validation," *J. Phys. Condens. Matter*, vol. 20, no. 20, pp. 204143, 2008. DOI: [10.1088/0953-8984/20/20/204143](https://doi.org/10.1088/0953-8984/20/20/204143).
- [13] H. Ki, "Level set method for two-phase incompressible flows under magnetic fields," *Comput. Phys. Commun.*, vol. 181, no. 6, pp. 999–1007, 2010. DOI: [10.1016/j.cpc.2010.02.002](https://doi.org/10.1016/j.cpc.2010.02.002).
- [14] M. Habera and J. Hron, "Modelling of a free-surface ferrofluid flow," *J. Magn. Magn. Mater.*, vol. 431, pp. 157–160, 2017. DOI: [10.1016/j.jmmm.2016.10.045](https://doi.org/10.1016/j.jmmm.2016.10.045).
- [15] S. Afkhami, Y. Renardy, M. Renardy, J. Riffle, and T. Pierre, Numerical modeling of ferrofluid droplets in magnetic fields, presented at the AIP Conference Proceedings, vol. 1027, pp. 884–886, 2008.
- [16] S. Afkhami *et al.*, "Deformation of a hydrophobic ferrofluid droplet suspended in a viscous medium under uniform magnetic fields," *J. Fluid Mech.*, vol. 663, pp. 358–384, 2010. DOI: [10.1017/S0022112010003551](https://doi.org/10.1017/S0022112010003551).
- [17] D. Shi, Q. Bi, and R. Zhou, "Numerical simulation of a falling ferrofluid droplet in a uniform magnetic field by the VOSET method," *Numer. Heat Transf. Part A Appl.*, vol. 66, no. 2, pp. 144–164, 2014. DOI: [10.1080/10407782.2013.869459](https://doi.org/10.1080/10407782.2013.869459).
- [18] A. Ghaffari, S. Hashemabadi, and M. Bazmi, "CFD simulation of equilibrium shape and coalescence of ferrofluid droplets subjected to uniform field," *Collid. Surf. A Physicochem. Eng. Asp.*, vol. 481, pp. 186–198, 2015. DOI: [10.1016/j.colsurfa.2015.04.038](https://doi.org/10.1016/j.colsurfa.2015.04.038).
- [19] P. Capobianchi, M. Lappa, and M. Oliveira, "Deformation of a ferrofluid droplet in a simple shear flow under the effect of a constant magnetic field," *Computer. Fluids*, vol. 173, pp. 313–323, 2018. DOI: [10.1016/j.compfluid.2018.06.024](https://doi.org/10.1016/j.compfluid.2018.06.024).
- [20] J. Liu, S. Tan, Y. Yap, M. Ng, and N. Nguyen, "Numerical and experimental investigations of the formation process of ferrofluid droplets," *Microfluid Nanofluid*, vol. 11, no. 2, pp. 177–187, 2011. DOI: [10.1007/s10404-011-0784-7](https://doi.org/10.1007/s10404-011-0784-7).
- [21] J. Liu, Y. Yap, and N. Nguyen, "Numerical study of the formation process of ferrofluid droplets," *Phys. Fluids*, vol. 23, no. 7, pp. 072008, 2011. DOI: [10.1063/1.3614569](https://doi.org/10.1063/1.3614569).
- [22] U. Sen *et al.*, "Dynamics of magnetic modulation of ferrofluid droplets for digital microfluidic applications," *J. Magn. Magn. Mater*, vol. 421, pp. 165–176, 2017. DOI: [10.1016/j.jmmm.2016.07.048](https://doi.org/10.1016/j.jmmm.2016.07.048).

- [23] M. Aboutalebi, M. Bijarchi, M. Shafii, and S. Hannani, "Numerical investigation on splitting of ferrofluid microdroplets in t-junctions using an asymmetric magnetic field with proposed correlation," *J. Magn. Magn. Mater.*, vol. 447, pp. 139–149, 2018. DOI: [10.1016/j.jmmm.2017.09.053](https://doi.org/10.1016/j.jmmm.2017.09.053).
- [24] V. Varma *et al.*, "Control of ferrofluid droplets in microchannels by uniform magnetic fields," *IEEE Magn. Lett.*, vol. 7, pp. 1–5, 2016, DOI: [10.1109/LMAG.2016.2594165](https://doi.org/10.1109/LMAG.2016.2594165).
- [25] A. Ray *et al.*, "Magnetic droplet merging by hybrid magnetic fields," *IEEE Magn. Lett.*, vol. 7, pp. 1–5, 2016. DOI: [10.1109/LMAG.2016.2613065](https://doi.org/10.1109/LMAG.2016.2613065).
- [26] M. Hassan, J. Zhang, and C. Wang, "Deformation of a ferrofluid droplet in simple shear flows under uniform magnetic fields," *Phys. Fluids*, vol. 30, no. 9, pp. 092002, 2018.
- [27] A. Ghaderi, M. Kayhani, and M. Nazari, "Numerical investigation on falling ferrofluid droplet under uniform magnetic field," *Eur. J. Mech. B Fluids*, vol. 72, pp. 1–11, 2018. DOI: [10.1016/j.euromechflu.2018.04.008](https://doi.org/10.1016/j.euromechflu.2018.04.008).
- [28] D. Sun and W. Tao, "A coupled volume-of-fluid and level set (VOSET) method for computing incompressible two-phase flows," *Int. J. Heat Mass Transf.*, vol. 53, no. 4, pp. 645–655, 2010. DOI: [10.1016/j.ijheatmasstransfer.2009.10.030](https://doi.org/10.1016/j.ijheatmasstransfer.2009.10.030).
- [29] K. Ling, Z. Li, D. Sun, Y. He, and W. Tao, "A three-dimensional volume of fluid & level set (VOSET) method for incompressible two-phase flow," *Comput. Fluids*, vol. 118, pp. 293–304, 2015. DOI: [10.1016/j.compfluid.2015.06.018](https://doi.org/10.1016/j.compfluid.2015.06.018).
- [30] G. Tryggvason, R. Scardovelli, and S. Zaleski, *Direct Numerical Simulations of Gas-Liquid Multiphase Flows*. Cambridge: Cambridge University Press, 2011.
- [31] J. Brackbill, D. Kothe, and C. Zemach, "A continuum method for modeling surface tension," *J. Comput. Phys.*, vol. 100, no. 2, pp. 335–354, 1992. DOI: [10.1016/0021-9991\(92\)90240-Y](https://doi.org/10.1016/0021-9991(92)90240-Y).
- [32] W. Lee, R. Scardovelli, A. Trubatch, and P. Yecko, "Numerical, experimental, and theoretical investigation of bubble aggregation and deformation in magnetic fluids," *Phys. Rev. E*, vol. 82, pp. 016302, 2010.